Fluorescence Depolarization Investigation of the Lobed Jet 90° Twists and Structural Features

Cristina M. Quintella,* Ana Paula S. Musse, and Cristiane C. Gonçalves

Instituto de Química, Universidade Federal da Bahia, Campus Universitario de Ondina, CEP: 40.170-290, Salvador, BA, Brazil

Received: May 5, 2003; In Final Form: November 26, 2003

Although lobed jets have been known for over 60 years, the causes behind their lobes generation and 90° twist has not yet been elucidated. Four vertical ethylene glycol jets were generated by 300 or 500 μm thick slit nozzles. The jets showed six lobes twisted 90° one from another. The odd and the even lobes were in the frontal and lateral planes, respectively. For each jet, the length of the lobes increased with volumetric rate while their number remained constant. Polarization maps of molecular alignment for frontal and lateral views were acquired by fluorescence depolarization (0.01 mm^2 resolution). Upon their integration, velocity maps were obtained. These allowed to identify at the top of each lobe two lateral divergent inner streams that converge at the bottom. Then they merged, generating the next lobe at exactly 90°. This pattern repeated itself producing the consecutive lobes. Additionally, the polarization maps showed that lobed jets may be suitable to control molecular alignment reactions as they provide quite defined regions of high or low molecular alignment (within each lobe) and have efficient molecular mixing at the merging points (between the lobes).

1. Introduction

Liquid jets are of significance in fundamental hydrodynamic research, in analytical methods, in engineering processes, and in nature itself. By fully characterizing such jets, it may be possible to increase equipment performance and reaction yields since they are widely used for cooling reactor walls and in generating sprays, for example. A well-known feature of liquid jets is the lobed structure they adopt in which successive regions are turned through 90° relative to the preceding and the following regions. The lobes result from competition between inertial and viscous forces within the jet and vary in dimension as distance from the jet nozzle increases before they finally merge to a cylindrical shape. Both experiment and simulation methods have been used to characterize the geometry and flow regime of liquid jets though the origin of the distinctive lobed structure at the molecular level seems to have received little attention.

In a series of experimental papers, we have sought a molecular level understanding of the structure and properties of planar liquid jets[1,2] both inside and outside the jet nozzle[3] by mapping the depolarization of probe molecule fluorescence over the surface of the planar regions. The aim of the study reported here has been to elucidate the mechanism of lobe formation, the reason for their striking 90° rotation relative to the preceding lobe, and to probe this hydrodynamic behavior at the molecular level. The experimental technique used is the depolarization of laser-induced fluorescence presented here in the form of 2-D maps of the degree of depolarization for four of the lobes formed by a planar liquid jet. The polarized fluorescence technique was used to investigate liquid motion in the lobes both frontally and laterally. Relative velocity maps were obtained by functional integration of each profile of the polarization maps. The results suggest that fluorescence depolarization is a useful experimental technique for characterizing thin liquid flows used in technological processes as well as to elucidate the intermolecular alignment behind chemical processes. This appears to be the first time that fluorescence depolarization has been mapped for the structured regions of lobed jets.

1.1 The Lobed Jet. The lobed jet exists only within a specific range of Reynolds numbers (Re), and therefore is strongly dependent on such factors as nozzle geometry, viscosity, surface tension, temperature, pressure, and so forth. One of the earliest systematic studies of free thin liquid jets was reported by Andrade[4] and concerned dependence of jet stability on Re. The 1950s saw a growth of interest in airborne liquid jets (free jets) particularly in their disintegration for in-spray formation.[5−7] Härri et al.,[8] in search of the best design for dye laser nozzles, derived a Re expression for thin slit nozzles that produce lobed jets with steady laminar flow over the initial region and found that the ratio between the smallest slit dimension and the nozzle length should be greater than 0.06 Re for optimum performance.

Lobed jets have been described as oscillating jets[9] or as plane jets (when only the first lobe was considered).[10] The edges of the first lobe have been referred to as asymmetric waves and in other descriptions the lobes are referred to as lenses[7] or as having bone-shaped profiles.[1,2] Lord Raleigh (1879)[11] proposed a method of monitoring surface tension on the basis of the progressive reduction of lobe width, and this has been used since then to determine the dynamic evolution of surface tensions of different solutions.[9] Recently, Elwell et al.[12] reported the use of oscillating first lobes to shield walls of inertial fusion reactors from damaging particles.

1.2 Steady-State Fluorescence Depolarization. Liquids are characterized by strong intermolecular forces that account for macroscopic properties such as viscosity and surface tension. Within a liquid jet, friction between molecules moving at different speeds gives rise to viscous drag and shear forces associated with this drag to produce velocity gradients which,

* To whom correspondence should be addressed. E-mail: cristina@ufba.br; tel.: 55-71-99870188; fax: 55-71-2355166.

10.1021/jp035218x CCC: $27.50
Published on Web 01/31/2004

depending on flow conditions, nature of liquid, and so forth, may be accompanied by alignment of the molecules of the fluid.[13] A technique known for several decades to be a sensitive probe of molecular alignment is fluorescence depolarization.[14] Nonspherical fluorescent probe molecules become aligned within aligned host species such as flowing liquid molecules and the degree of alignment may be used as a sensor of velocity gradients within the flowing liquid.[1,2]

In an experimental determination, the polarization of fluorescence from a probe species within the flow is compared to that of the incident laser radiation. The characteristic rotational diffusion time within solvents of moderate viscosity such as ethylene glycol and probe excited-state lifetime are of similar order of magnitude[15] which makes fluorescence depolarization a method that is sensitive to intermolecular alignment. By making such measurements over all accessible regions of flowing liquid (i.e., polarization mapping), the degree of alignment of probe species may be quantified and the presence of velocity gradients within the host liquid that give rise to this alignment identified.

Fluorescence depolarization data can be interpreted as a bidimensional phenomenon in terms of polarization (P):[1,2,16]

$$P = \frac{I_{//} - I_{\perp}}{I_{//} + I_{\perp}}$$

where $I_{//}$ and $I_{\perp}$ are, respectively, the fluorescence components parallel and perpendicular to the axis defined by the direction of laser polarization. The probability the probe species will absorb laser light polarized along this principal axis is proportional to the square cosine of the angle between the probe molecule's transition dipole and the laser beam polarization. Thus, molecules aligned mainly in this vertical direction will interact with laser light and be photoselected. During the excited lifetime, molecules may or may not remain in their original orientations depending on their movement freedom within the liquid. This freedom depends on the anisotropic rotational diffusion of dye molecules and on the shear field intensity within the liquid flow.

If the probe molecules are in a region of high shear, that is, highly aligned molecular domains, the probe species will remain aligned and, on radiative decay, the fluorescence emission will primarily be in the direction of the original polarization of excitation. If the shear forces are small, however, molecular domains will rapidly lose their alignment and the liquid molecules will have no preferential alignment direction, causing the scrambling of probes alignment, with no well-defined direction of fluorescence polarization.

1.3 Studies of Fluorescence Depolarization within Liquid Flows. There have been relatively few experimental studies of the molecular hydrodynamics of liquid flows in which fluorescence depolarization has been the principal method of investigation. Kenyon et al.[1,2] showed that the central part of the first lobe of a lobed jet has a nonhomogeneous pattern of molecular alignment and qualitatively obtained velocity profiles through integration of the polarization profiles. Quintella et al.[3] obtained polarization maps for ethylene glycol flow (Re = 90) inside a quartz slit nozzle and outside at the first lobe of a free thin jet, determining, by direct visualization at a molecular level, the boundary layers. These authors functionally integrated the polarization profiles obtaining the velocity map over the flow studied.

Bain et al.[15,17] used time-correlated-single-photon counting to study depolarization kinetics with picosecond time resolution within some regions of the first lobe of a free thin jet and found that the rotational diffusion rates parallel and perpendicular to the flow vary by up to 10% depending on the region probed. Gonçalves[18] and Quintella et al.[19] used previous data[1−3] to validate an experimental setup developed and built to acquire fluorescence depolarization within liquid flows. Recently, Quintella et al. demonstrated that fluorescence depolarization within a liquid free flowing film on a solid surface can give information on the dynamic interfacial tension and that it is sensitive to the chemical composition of the flowing liquid,[19] its interaction with the surface,[20] and the orientation of molecular groups on the surface.[21] These authors also demonstrated that it is possible to obtain further information on the surface chemical composition by this method[22] when comparison is made with static methods such as the contact angle.[11] A recent application demonstrates the usefulness of this method in determining microscopic changes of the chemical constitution of the inner walls of microflow cells.[23]

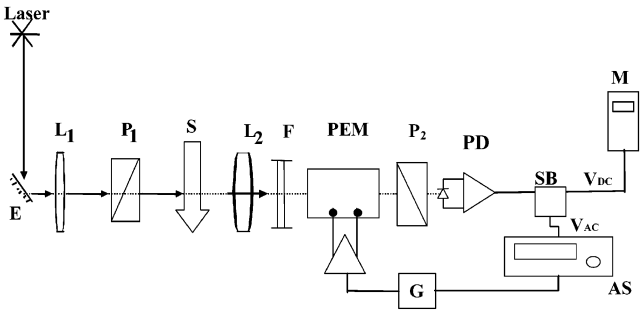

Figure 1. Scheme of the experimental setup to map the liquid intermolecular alignment using fluorescence depolarization. L1: biconvex lens; P1: vertical polarizer; L2: biconvex lens; F: 570 nm orange high pass filter; PEM: photoelastic modulator; P2: vertical polarizer; PD: photodiode; SB: splitter box to split the V_{AC} and the V_{DC} signals; *G*: frequency generator; AS: lock-in amplifier.

2. Experimental Section

2.1 Fluorescence Depolarization (PLF) Setup. The experimental arrangement was previously described by Kenyon et al.[1,2] (Figure 1). Briefly, a 514.5 nm vertically polarized laser beam at 70 mW is focused by lens L1. Lens L2 focuses the fluorescence on to photodiode PD, through a photoelastic modulator PEM, a horizontal polarizer P2, and an orange filter F. The signal is split into the V_{AC} and V_{DC} components. The polarization is given by the ratio between the difference between V_{AC} and V_{DC} and their sum.[1,2] A correction factor for optical components birefringence was used.

2.2 PLF Controls. The liquid under investigation here is ethylene glycol into which is seeded a low concentration (9×10^{-3} mol L^{-1}) of the fluorescent probe Rhodamine 6G (R6G) obtained from Lambda Physik (99.99% purity). This is a xanthene dye with good photochemical stability and high fluorescence quantum yield. It is a "T" shaped molecule with a planar backbone and a perpendicular out-of-plane ring. In solution, it loses the chloride ion and leaves a positive charge on one of the nitrogen atoms. When excited at 514.5 nm, it is pumped from S_0 to S_1 state.[24] This transient charge oscillates along the molecular "backbone". The molecule returns to its lowest electronic state by fluorescent emission with a transition dipole moment that is polarized parallel to the long axis of the molecule.[25]

When using the fluorescence depolarization technique, the choice of probe molecule concentration is critical to avoid quenching processes and to maximize signal-to-noise ratio. In highly concentrated solutions, intermolecular transfer of the

TABLE 1: Experimental Parameters of Ethylene Glycol Lobed Jets: Jet Net Velocity, Slit Nozzle Width, and Reynolds Number (Re)

jet	slit width (μm)	Re[a]	jet net velocity (m s^{-1})
1	300	68	2.30
2	300	96	3.26
3	300	124	4.20
4	500	86	1.76

[a] Formula from ref 8.

excitation energy may take place through inductive fields, a short-range resonant process.[26,27] For R6G dissolved in ethylene glycol (MEG), the concentration for this effect to become negligible is around 10^{-2} g cm^{-3}. High concentrations also give rise to concentration quenching. This self-quenching is due to dimerization or complex formation.[27] For R6G dissolved in ethylene glycol, the strong repulsion between positively charged moieties in ethylene glycol inhibits dimerization, causing dimers to form only at concentrations above[28] 10^{-2} mol L^{-1}, which is 2 orders of magnitude higher than in water or methanol. For a fluorescent molecule to be an effective probe of molecular alignment, its rotational diffusion time and excited lifetime must be of similar order of magnitude. Scully et al.[27] found that, for a solution in our conditions, the excitation lifetime is $\sim 10^{-9}$ s and the rotational diffusion time has been measured at $\sim 2 \times 10^{-9}$ s.[15,17]

In the experiment reported here, fluorescence polarization readings were made within the flowing liquid for several values of laser power to eliminate the possibility of optical pumping. Such effects were negligible even for laser power of the order of 500 mW. The measurements were independent of the total fluorescence intensity over the range studied here. Fluorescence polarization values acquired at defined control points before and after experiments were repeatable to within 0.2%.

2.3 Lobed Jets. Two different sapphire nozzles were used to produce the liquid jets, and these developed the highly distinctive lobed structures that coalesce and reform as lobes twisted through 90° relative to the previous lobe. The nozzles consist of high precision devices manufactured from crystalline sapphire optically flat polished to a flatness of less than 1 μm and separated by Teflon spacers that define the aperture size and geometry.[8] They have channel length of 40 mm and slit apertures of 6 mm $\times$ 300 μm and 6 mm $\times$ 500 μm. The liquid jet consists of Merck 99.5% ethylene glycol (MEG), chosen for its physical properties such as viscosity and low evaporation rate and widely used in fluorescence depolarization studies.[1,2,19,29] The liquid's temperature was kept at (14.0 $\pm$ 0.2) °C. Jet net velocities were obtained by dividing the volumetric rate by the nozzle channel area. They ranged from (176 $\pm$ 5) to (420 $\pm$ 5) cm s^{-1}. Table 1 shows the experimental parameters of the four studied jets. The fluid viscosity was measured for several fluorescent probe concentrations by the Ostwald method and a second-order curve was fitted to the data and under the conditions of the experiments reported here was 0.224 g cm^{-1} s^{-1}. The Re ranged from[8] 68 to 124 and critical[30] Re is 1000, and so these flows are all classified as laminar.

In the experiment, the nozzle is held in a two-axis linear translation stage and moved in a plane perpendicular to the laser beam, so as to scan the laser either across the jet (lateral scan with accuracy of 5×10^{-2} mm) or along the jet (vertical scan with accuracy of 2×10^{-1} mm). To move from frontal view to lateral view, the nozzles and, consequently the jets, were rotated 90° around the vertical axis.

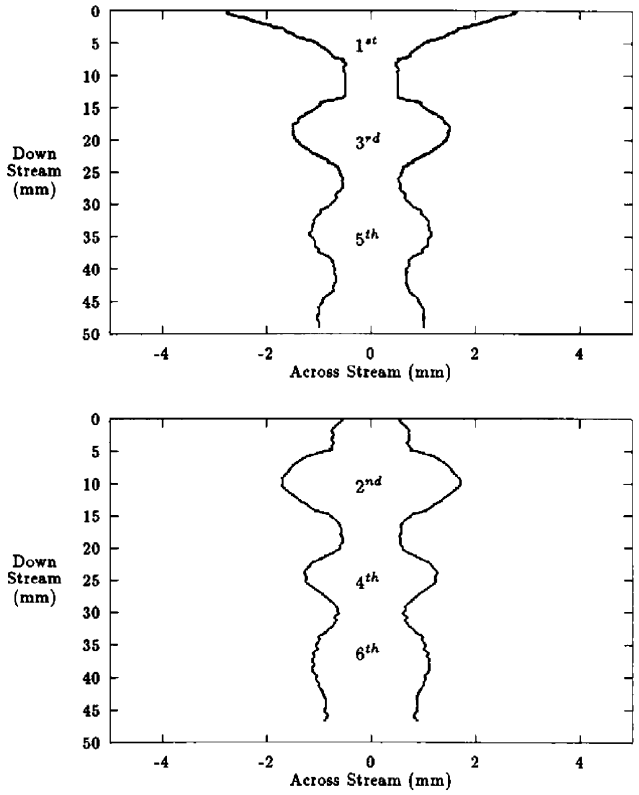

Figure 2. Boundaries of jet 4 (see Table 1) showing lobe numbers. Top: frontal contour. Bottom: lateral contour.

3. Results and Discussion

3.1 Jet Shapes. Three basic shapes may be generated within the liquid jet by varying only the downstream net velocity with all other experimental conditions remaining unchanged. At low velocity, the jet consists of a short, triangular thin liquid sheet that becomes a cylindrical thread almost immediately after exiting the nozzle. As velocity is increased, the lobed structure develops more fully and five lobes could clearly be seen with some evidence of a sixth. The length of each lobe increased with velocity, though their number remained constant. Lobes further down stream were less wide, tending to a rod shape, suggesting occurrence of a lateral damping process. As velocity is further increased, the jet, near the nozzle, splits into two divergent, nearly cylindrical, threads of fluid that tend to break down into either several drops or threads. For the measurements reported here, the liquid velocity was chosen so that stable, well-defined lobe structures were produced.

Four different jets, each having well-developed lobed structure, were studied and their properties are summarized in Table 1. All exhibited quite similar shapes. Each jet had consecutive lobes that were rotated exactly by 90° relative to neighbor lobes. Odd and even lobes were, respectively, in the frontal and lateral planes. Exact jet contours along all its extension (Figure 2) were determined when the angle between incident laser beam and its scattered light was 90°. Laser scatter showed that lateral profiles at the downstream positions between consecutive lobes had the shape of a cross with branches in frontal and lateral planes.

3.2 Polarization Maps. Fluorescence polarization measurements were made across and down the flow from the point at which liquid emerges from the nozzle to the end of the lobed structure of the jet and these measurements would typically be made within a single day for each jet. Kenyon et al.[1,2] have described the procedure for acquisition of fluorescence depo-

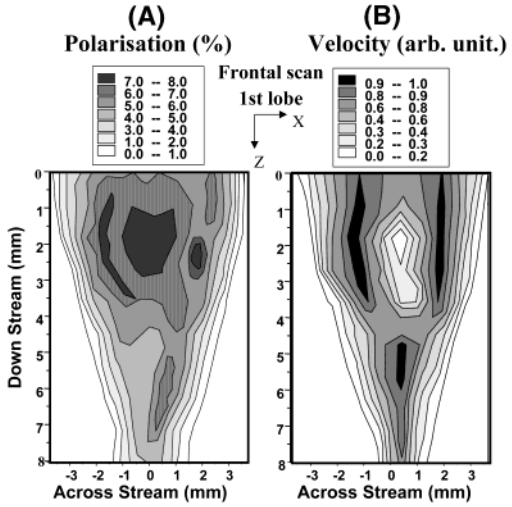

Figure 3. Maps obtained for the 1st lobe of jet 1 (see Table 1): (A) map of polarization showing the intermolecular alignment within the liquid jet; (B) map of juxtaposed velocity obtained by integration of polarization profiles.

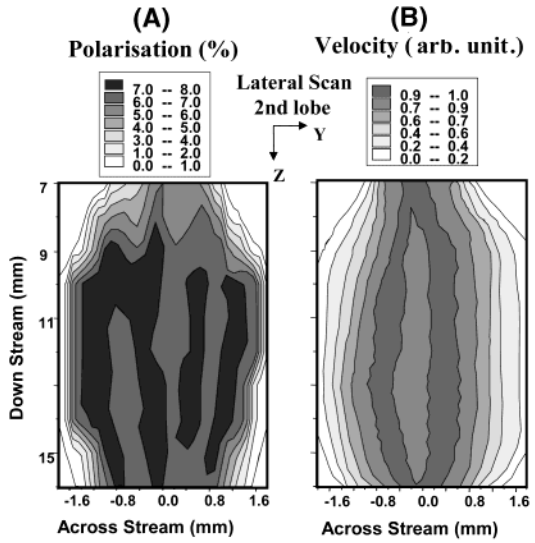

Figure 4. Maps obtained for the 2nd lobe of jet 1 (see Table 1): (A) map of polarization showing the intermolecular alignment within the liquid jet; (B) map of juxtaposed velocity obtained by integration of polarization profiles.

larization maps of fluid emerging from a slit jet in a frontal scan of the middle section of the first lobe. Polarization measurements were made both across the flat frontal odd-numbered lobes (*ZX* plane, averaging the narrow *Y* dimension) and across the flat lateral even-numbered lobes (*ZY* plane), that is, averaging over the narrow *X* dimension. The liquid flow was scanned both frontally by acquiring polarization profiles $P_z(x)$ across the stream (*X*) at consecutive positions down the stream (*Z*) and laterally by acquiring polarization profiles $P_z(y)$ across the stream (*Y*).

Figures 3A and 4A illustrate the polarization maps for two of the lobes acquired. All lobes except the first one have broadly similar polarization patterns. The first lobe had polarization patterns clearly related to the following lobes. Net polarization increased as the distance downstream increased, that is, for the higher order lobes.

3.3 Velocity Maps. The alignment of fluorescent probe molecules in a flowing liquid results from the shear forces that are generated by streams within the flowing liquid that are traveling at different speeds and is sensitive to the viscous drag that generates these shear forces. We have demonstrated[3] that it is possible to determine velocity distributions from the polarization maps since the shear forces can be seen as the first velocity differential with respect to one abscissa (Massey 1989).[13] Velocity maps (on a relative scale) were obtained by simple data treatment of each polarization profile using the methodology previously described.[3] For the frontal scans, initially each of the downstream polarization profiles obtained experimentally across the stream was fitted by a sum of *n* Gaussian curves.

$$\text{Frontal: } P_Z(x) = \sum_{i=1}^{n} g_{Zi}(x) \qquad \text{Lateral: } P_Z(y) = \sum_{i=1}^{n} g_{Zi}(y)$$

where *n* is the number of maxima in each polarization profile. Although there are experiments that distinguish between up and down polarization, our experimental method does not. To lift this degeneracy, the even-numbered Gaussians (corresponding to the modulus of negative velocity gradients) were inverted and new curves were constructed, corresponding to the gradient of velocity.

$$\text{Frontal: } F_Z(x) = \sum_{i=1}^{n} (-1)^{i+1} g_{Zi}(x)$$

$$\text{Lateral: } F_Z(y) = \sum_{i=1}^{n} (-1)^{i+1} g_{Zi}(y)$$

Finally, the resulting functions were integrated yielding the velocity profiles.

Calibration of the velocity profiles is not straightforward. The volumetric rate flow is constant and the average downstream velocity can also be considered constant (according to measurements by Bain et al.[15] it varies by less than 2%). However, the shape of the lateral cross section (plane *XY*) changes along the flow and the measurement averages along the thinnest width of the jet (*X* and *Y*, respectively, for lateral and frontal scans). Without knowing the precise dimensions of the cross section for each downstream position, it is not possible to calibrate the velocity; thus, each velocity profile has its own arbitrary units. The juxtaposing of the profiles is illustrated in Figures 3B and 4B.

3.4 Discussion. In the frontal view of the first lobe (Figure 3A), soon after emerging from the nozzle, the polarization of the probe molecules is almost constant in the central region, though four small maxima may be discerned in the data. These maxima gradually increase (from 0 to 2.5 mm downstream). Integration of the velocity map indicates the presence of two principal streams coexisting within the jet (Figure 3B). These streams begin to converge (2.5−4.5 mm downstream) and the first lobe becomes triangular in shape. The streams then merge and only one can be observed in the frontal view (Figure 3B, after 4.5 mm downstream). The lateral view obtained in the second lobe (Figure 4A) begins with two polarization maxima that separate further downstream to become four divergent maxima (8.0−12.0 mm downstream), corresponding to two divergent inner velocity streams (Figure 4B). Then, these two inner streams converge until they become only one inner stream. Thus, the first lobe might be viewed as a process that follows the development of the second half of a full lobe.

This pattern of lateral internal streams that build up during the first half of the lobe and then converge in the second half repeats itself from lobe to lobe for all four jets examined here. At the bottom of each lobe and at the beginning of the next,

the internal streams are merging and only an average of both frontal and lateral lobes is detected. They then develop the characteristic structure further, producing a perpendicular liquid sheet (the next lobe) in a manner similar to the well-known sheet generated by two colliding heads-on jets.[31] The lateral jet profile at this intersection, as determined by scattered laser light, confirms this interpretation since it consists of a cross with arms in the frontal and lateral directions. Each pair of arms corresponds to the lobe that ends and the lobe that is starting, respectively. Thus, each 90° twist is the result of the merging of two inner streams at the bottom of each lobe and the beginning of the next lobe.

On emerging from the nozzle, the absence of wall and the very small viscous drag at the glycol−air interface causes asymmetric interactions at the jet boundary (liquid−air), producing strong surface tension forces in the lateral direction upon the edge molecules. These are relatively short-range forces and are not experienced by molecules in the middle of the jet. This internal pull causes molecules in the edge to move gradually toward the center.

The next lobe was less wide than the previous one and may be explained by loss of lateral movement total energy, because of the drag of viscous forces, specially the ones involved in the collision of internal streams. This justifies the use of lobed jets to evaluate surface tension of different chemical components.

As the lateral movement is becoming damped, the resultant force acting on jet molecules is becoming more vertically orientated. Thus, the downstream orientation of molecular domains is increasing, explaining the net polarization increase observed experimentally for the higher order lobes.

The observation that the lobes are stretched as jet velocity increases suggests that the downstream position (millimeters) could be labeled as jet existence time (milliseconds).

4. Conclusions

In this work, we report a study of lobe-forming liquid jets of ethylene glycol emerging from narrow slit-shaped nozzles. The properties of four of the lobes were mapped in detail, their structural features by high precision laser scattering and the alignment of probe molecules within the flow by fluorescence depolarization. It was observed that increase in jet velocity elongates the lobes but does not change their number.

By integration of the polarization maps along lateral abscissa, it was possible to obtain velocity distributions along and down the jet. This allowed us to infer velocity profiles and to discuss macroscopic fluid dynamical concepts in terms of interactions between the molecules of the flowing liquid. It was observed that each lobe of the jet has two internal streams that arise at the beginning of the lobe, then converge at the bottom, reducing lobe width, and finally merge, generating the next lobe, exactly at 90°.

These insights into molecular interactions within liquid flows may be of value in controlling chemical reactions since streams within the jet contain molecules that are partially aligned; further, they may be controllably mixed at points within the jet's development. This may be of value in laboratory or industrial processes.

Acknowledgment. We thank Conselho Nacional de Desenvolvimento Científico e Tecnológico (CNPq, Brazil) for grants. A.P.S.M. acknowledges an undergraduate research fellowship from PIBIC-CNPq and CNPq. C.C.G. acknowledge a DPhil scholarship from CAPES.

References and Notes

(1) Kenyon, A. J.; McCaffery, A. J.; Quintella, C. M. *Mol. Phys.* **1991**, *72*, 965.
(2) Kenyon, A. J.; McCaffery, A. J.; Quintella, C. M.; Winkel, J. F. *Mol. Phys.* **1991**, *74*, 871.
(3) Quintella, C. M.; Gonçalves, C. C.; Musse, A. P. S.; McCaffery, A. J. *Exp. Fluids* **2003**, *35(1)*, 41.
(4) Andrade, E. N. C. *Proc. Phys. Soc.* **1939**, *51*, 784−793.
(5) Squire, H. B. *Brit. J. Appl. Phys.* **1953**, *4*, 167−169.
(6) Fraser, R. P.; Dombrowski, N.; Eisenklam, P. *Nature* **1954**, *173*, 495.
(7) Taylor, G. I. *Proc. R. Soc. London A* **1959**, *253*, 313−321.
(8) Härri, H.; Lentwyler, S.; Schumacher, E. *Rev. Sci. Instrum.* **1982**, *53*, 1855−1858.
(9) Bechtel, S. E.; Koelling, K. W.; Nguyen, W.; Tan, G. *J. Colloid Interface Sci.* **2002**, *245*, 142−162.
(10) Adachi, K. *J. Non-Newtonian Fluid Mech.* **1987**, *24*, 11−30.
(11) Adamson, A. W.; Gast, A. P. *Physical Chemistry of Surfaces*; John Wiley & Sons Inc.: New York, 1997.
(12) Elwell, L. C.; Sadowski, D. L.; Yoda, M.; Abdel-Khalik, S. I. *Fusion Technol.* **2001**, *39*, 716−720.
(13) Massey, B. S. *Mechanics of Fluids*, 6th ed.; Van Nostrand: Wokingham, UK, 1989.
(14) Feofilov, P. P *The Physical Basis of Polarized Emission*; Consultants Bureau: New York, 1961.
(15) Bain, A. J.; Chandna, P.; Butcher, G.; Bryant, J. *J. Chem. Phys.* **2000**, *112*, 10418−10434.
(16) Kawski, A. *Crit. Rev. Anal. Chem.* **1993**, *23*, 459.
(17) Bain, A J.; Chandna, P.; Butcher, G. *Chem. Phys. Lett.* **1996**, *260*, 441−446.
(18) Gonçalves, C. C. *Desenvolvimento da Técnica de PLF e sua Aplicação para o Estudo do Alinhamento Intermolecular de Sistema Dinâmicos*; Instituto de Química, UFBA: Salvador, Brazil, 2000.
(19) Quintella, C. M.; Gonçalves, C. C.; Pepe, I.; Lima, A. M. V.; Musse, A. P. S. *J. Autom. Methods Manage. Chem.* **2002**, *24*, 31−39 (available on line in English at http://taylorandfrancis.metapress.com).
(20) Quintella, C. M.; Gonçalves, C. C.; Pepe, I.; Lima, A. M. V.; Musse, A. P. S. *J. Braz. Chem. Soc.* **2001**, *12*, 780−786 (available on line, in English, at http://jbcs.sbq.org.br/jbcs/2001/vol12_n6/14.pdf).
(21) Quintella, C. M.; Lima, Â. M. V.; Gonçalves, C. C.; Watanabe, Y. N.; Schreiner, M. A.; Mammana, A. P; Pepe, I.; Pizzo, A. M. *J. Colloid. Interface Sci.* **2002**, *26(1)*, 221.
(22) Quintella, C. M.; Musse, A. P. S.; Castro, M. T. P. O.; Gonçalves, C. C.; Watanabe, Y. N. *J. Phys. Chem.* **2003** (submitted).
(23) Quintella, C. M.; Lima, Â. M. V.; Mammana, A. P; Schreiner, M. A.; Pepe, I.; Watanabe, Y. N. *J. Colloid. Interface Sci.* **2003** (in press).
(24) Aristov, A. V.; Shevandin, V. S. *Opt. Spectrosk.* **1977**, *43*, 228−232.
(25) Penzkofer, A.; Wiedmann, J. *Opt. Commun.* **1980**, *35*, 81−86.
(26) Föster, T. *Ann. Phys.* **1948**, *2*, 55−75.
(27) Scully, A.; Matsumoto, A.; Hirayama, S. *Chem. Phys.* **1991**, *157*, 253−269.
(28) Bojarski, P.; Matczuk, A.; Bojarski, C.; Kawski, A.; Kuklinski, B.; Zurkowska, G.; Diehl, H. *Chem. Phys.* **1996**, *210*, 485−499.
(29) Quintella, C. M.; Gonçalves, C. C.; Castro, M. T. P. O.; Pepe, I.; Musse, A. P. S.; Lima, Â. M. V. J. *Phys. Chem. B* **2003**, *107(33)*, 8511.
(30) Bond, W. N. *Proc. Phys. Soc.* **1935**, *47*, 549−558.
(31) Brom, G. *R133/76;* Institut Franco-Allemand de Recherches de Saint-Louis: Saint Louis, France, 1976.